Numerical Simulation of Arterial Plaque Ruptures

A. Ferrara, A. Pandolfi

Politecnico di Milano Piazza Leonardo da Vinci 32, 20133 Milano (Italy)
URL: http://www.stru.polimi.it e-mail: aferrara@stru.polimi.it; pandolfi@stru.polimi.it

ABSTRACT: We present three-dimensional finite element simulations of damaged arteries, used to investigate the influence of the geometry and tissue properties on the plaque rupture. We adopt a baseline geometry reconstructed from a contiguous set of *in vitro* magnetic resonance images of a damaged artery. The tree-layered artery wall is discretized with tetrahedral finite elements. The material of the layers is described with the hyperelastic fiber reinforced anisotropic model proposed by Holzapfel et al. [1]. The material properties are calibrated by fitting experimental data available in the literature. The physical interfaces between plaque and artery are modeled with cohesive elements, as well as the fracture surfaces induced by the mechanical action. The fracture surfaces are explicitly introduced in the model only when the tensile strength of the material is reached.

KEYWORDS: Human Arteries, Atherosclerotic Plaque, Anisotropy, Fracture, Finite Elements.

1 INTRODUCTION

Arterial walls are composite structures containing elastin, collagen, cells, and ground matrix. At microscopic level, the arterial wall shows a layered structure, composed of three concentric zones, intima, media, and adventitia, separated by elastic membranes. The intima, made of a single layer of endothelial cells embedded in extracellular matrix, is very thin; with aging and atherosclerosis it becomes thicker and stiffer, developing a more complex and heterogeneous structure. The media is the thickest layer. The collagen constituents of the media, aligned along the the circumferential direction with a very little dispersion, are arranged in repetitive lamellar concentric units. The outermost layer, the adventitia, is surrounded by loose connective tissue, and is characterized a network of dispersed collagen fibers. In the three layers, it is possible to identify the presence of a double set of equivalent and equi-oriented fibers, immersed in an isotropic ground matrix. The fiber organization confers to the material an orthotropic structure.

Atherosclerosis is a vascular disease, characterized by accumulation of lipids, collagen, muscle fibers, macrophages, calcium and necrotic tissue into the intima. In general, atherosclerosis proceeds to the formation of atherosclerotic plaque (core), that may cause partial occlusion of the lumen and reduce the blood flow (stenosis). In advanced lesions, the core may contain a lipid pool separated from the lumen by a fibrous cap of connective tissue. The rupture of the atherosclerotic plaque is a common cause of acute myocardial infarction and unstable angina. A crucial evolution of atherosclerosis is thrombosis, which may occur via endothelial erosion or by disruption – or tearing– in the cap of a lipid-rich plaque. Plaque rupture is observed at the areas where the peak stress exceeds the strength of the material. According to in-vitro tests, human atherosclerotic materials generally fracture under stresses exceeding 300 kPa. Thus the peak stress is often used as a predictor of the location of atherosclerotic plaque rupture.

In the following, we present a finite element model of a diseased artery and to reproduce numerically the damage and the rupture of the plaque under mechanical action.

2 FINITE ELEMENT MODEL

2.1 Material Model for the Arterial Wall

In the present approach the wall material is assumed hyperelastic. The strain energy function Ψ of the anisotropic material is decomposed into the sum of a volumetric part $\Psi_{\rm vol}$, function of the volumetric deformation $J = \det \mathbf{F}$, an isotropic part $\Psi_{\rm iso}$, representing the behavior of the ground matrix, and an anisotropic

part Ψ_{aniso}, which accounts for the presence of two embedded families of fibers [3]:

$$\Psi = \Psi_{\text{vol}}(J) + \Psi_{\text{iso}}\left(\overline{I}_1\right) + \Psi_{\text{aniso}}\left(\overline{I}_4, \overline{I}_6\right). \quad (1)$$

The isotropic part of the strain energy function Ψ_{iso} is a function of the first invariant $\overline{I}_1$ of the modified Cauchy-Green right tensor $\overline{\mathbf{C}} = J^{-2/3}\mathbf{C}$, while the anisotropic part is a function of the two pseudo-invariants $\overline{I}_4$ and $\overline{I}_6$ linked to two-fiber anisotropy [8]:

$$\overline{I}_4 = \mathbf{a} \cdot \mathbf{C}\mathbf{a} \qquad \overline{I}_6 = \mathbf{g} \cdot \mathbf{C}\mathbf{g}, \quad (2)$$

where the two unit vectors $\mathbf{a}$ and $\mathbf{g}$ denote the fiber directions in the reference configuration. The expressions of the strain energy functions assumed in the present applications are:

$$\Psi_{\text{vol}}(J) = \frac{K}{2} \ln J \quad (3)$$

where K is the bulk modulus of the material,

$$\Psi_{\text{iso}}\left(\overline{I}_1\right) = \frac{\mu}{2}\left(\overline{I}_1 - 3\right) \quad (4)$$

where μ is the shear modulus of the matrix, and

$$\Psi_{\text{aniso}}\left(\overline{I}_4, \overline{I}_6\right) = \frac{k_4}{2k}\left(\exp\left[k\left(\overline{I}_4 - 1\right)^2\right] - 1\right) + \frac{k_6}{2k}\left(\exp\left[k\left(\overline{I}_6 - 1\right)^2\right] - 1\right) \quad (5)$$

where k ia a dimensionless constant and k_4, k_6 are the stiffness moduli related to the collagen fiber sets. The specific form of the derived constitutive equation requires the definition of five material parameters K, μ, k, k_4, and k_6, whose interpretations can be partially based on the underlying histological structure. The material parameters used in the subsequent calculations have been calibrated on the basis of experimental results [4].

2.2 Cohesive Model

In cohesive theories, the displacement jump $\mathbf{\Delta}$ across a cohesive surface S plays the role of a deformation measure, while the tractions $\mathbf{T}$ furnish the work-conjugate stress measure. Assigned a deformation mapping φ to the body, the displacement jump pertaining to the two surfaces ($S^{\pm}$) facing the cohesive surface is given by

$$\mathbf{\Delta} = \varphi^{+} - \varphi^{-}. \quad (6)$$

The experimental evidence shows that the cohesive behavior is different for opening mode (I) and sliding modes (II and III). Following [5], we assume the existence of a free energy density Φ per unit undeformed area, restricting our analysis to isothermal processes. In order to describe anisotropic behaviors on the cohesive surfaces, we consider the following form of energy:

$$\Phi = \Phi(\Delta^n, \Delta^1, \Delta^2, q) \quad (7)$$

where q is an internal variable introduced to account for irreversibility. In (7) we enforce the dependence on the contravariant components of the displacement jump referred to the deformed principal directions of anisotropy on the cohesive surface. The principal anisotropy directions define an orthonormal basis in the reference configuration, but under a deformation mapping they are described by a general basis.

As a consequence of the first and second laws of thermodynamics, Φ acts as a potential for the cohesive tractions and the cohesive law follows in the form

$$\mathbf{T} = T^n\,\mathbf{n} + T^1\,\mathbf{m}_1 + T^2\,\mathbf{m}_2, \quad (8)$$

where $\mathbf{n}$, $\mathbf{m}_1$ and $\mathbf{m}_2$ denote the covariant basis vectors on the deformed cohesive surface and

$$T^n = \frac{\partial \Phi}{\partial \Delta^n}, \quad T^1 = \frac{\partial \Phi}{\partial \Delta^1}, \quad T^2 = \frac{\partial \Phi}{\partial \Delta^2}. \quad (9)$$

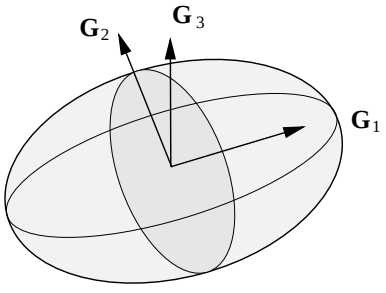

Figure 1: Resistance surface in the reference configuration. $\mathbf{G}_1$, $\mathbf{G}_2$, and $\mathbf{G}_3$ denote the principal anisotropy directions.

The orthotropic structure of the material assigns a different resistance to each direction. We generalize the anisotropic model used in Yu et al. [10] and introduce an ellipsoidal resistance surface, see Figure 1.

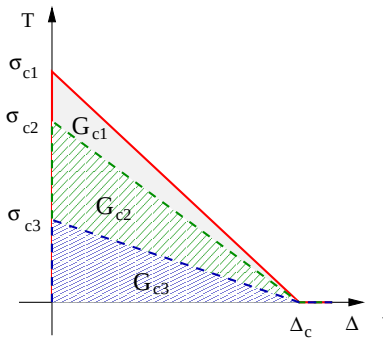

Figure 2: Set of cohesive laws considered in the present model. Cohesive strengths and critical energy release rates scale proportionally.

At each principal material direction is associated in general a different tensile resistance, i.e. $\sigma_{c1} \geq \sigma_{c2} \geq \sigma_{c3}$. We assume that the corresponding critical energy release rates are $G_{c1} \geq G_{c2} \geq G_{c3}$. The resistance of the material in the direction $\mathbf{N}$ is given by the solution of the system that represents the intersection of the chosen direction and the resistance ellipsoid, and will be expressed as $\sigma_c(\mathbf{N})$. The corresponding anisotropic cohesive law is characterized by a direction dependent scaling along the traction axis, see Figure 2. In order to decide about the insertion of a cohesive surface, at the end of each loading step, on every interelement surface, the "effective" traction T is computed as:

$$T = \sqrt{(T^n)^2 + \beta^{-2}\left[(T^1)^2 + \alpha^{-2}(T^2)^2\right]} \qquad (10)$$

where α and β are material parameters that account for anisotropy [5, 2]. Thus, the effective value is compared with the normal fracture resistance $\sigma_c(\mathbf{N})$:

$$T \leq \sigma_c(\mathbf{N}). \qquad (11)$$

If the fracture criterion (11) is violated, the topology of the mesh is updated with the creation of a new surface and the insertion of a cohesive element, using the algorithm described in [6]. The cohesive parameters used in the calculations have been obtained from the literature [7, 1].

2.3 Geometry and Finite Element Discretization

A three-dimensional model of a stenotic artery, reconstructed by manual segmentation of in-vitro high resolution magnetic images (MRI) [9], has been used in finite element simulations. The images reproduced transversal sections of a human arterial specimen, piled up along the arterial axis, at 1.2 mm distance one from the other, and identify four different zones: adventitia (A), media (M), intima plus plaque (I+P), and lipid pool (Lp).

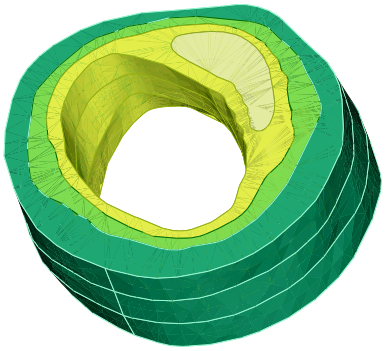

Figure 3: 3D view of a diseased artery consisting of adventitia, media, and deposit composed of the intima plus plaque and a lipid pool. The stenosis level is 40%.

The geometry represents an atherosclerotic lesion, with a stenosis of about 40%, characterized by an eccentric fibrous plaque and an extracellular lipid pool in the plaque core, see Figure 3. The model has been automatically discretized in 10-node tetrahedral elements, preserving the material distinction.

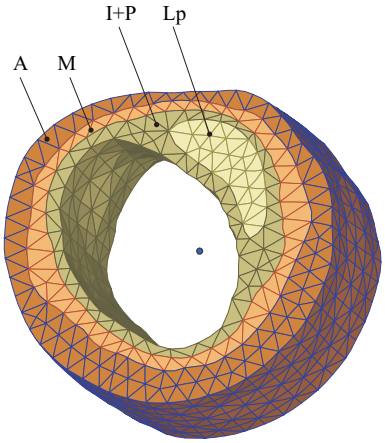

Figure 4: Finite element mesh: Adventitia (A), media (M), intima+plaque (IP), and lipid pool (Lp).

Figure 4 shows the finite element mesh, consisting of 8130 nodes and 4705 solid elements (tetrahedra). No cohesive elements are present in the original mesh to describe the interface between the layers.

3 NUMERICAL SIMULATIONS

We used a nonlinear finite element code explicitly developed for the static analysis of biological tissues and organs, equipped with fracture algorithms to simulate progressive rupture in anisotropic materials. For the analysis of the diseased artery we apply an axial prestretch, λ =1.2, to reproduce the in-situ conditions observed experimentally. The external confinement due to the surrounding tissues under normal physiological condition is simulated by applying an external uniform pressure growing progressively. In our simulations the blood pressure acting on the internal surface of the artery is uniformly applied by small quasi-static increments from 0 to 260 mmHg. Note that the physiological blood pressure oscillates in the range 80-120 mmHg.

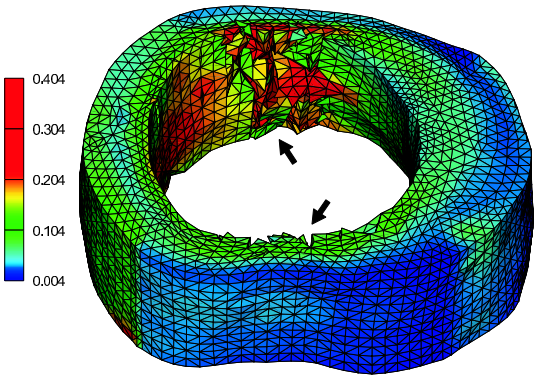

Figure 5: Mises stress map in MPa at 260 mmHg blood pressure.

Figure 5 shows the contour levels of the Mises stress at the end of the analysis. Our finite element analysis predicts that the rupture of the plaque originates from the intima, precisely at the shoulders of the diseased zone of the intima, where –under physiological conditions– the peak stress is observed. Cracks propagate in the radial direction across the intima layer, exposing the more resistant media layer to the lumen. Lateral side cracks are spread along longitudinal channels. As consequence of the crack propagation, the resistant section of the artery wall reduces. The simulations shows a reduction of the structural stiffness. Concentrations of stress are observed in correspondence of the narrowed walls.

4 CONCLUSIONS

The results obtained in this research represent a first step towards the development of a patient-specific computer assisted tool that may help surgeons in the prediction of the mechanical evolution of artery lesions. The numerical instrument already possesses the ability to evaluate quantitatively the stress field under strong mechanical actions, as the ones induced by balloon angioplasty or by a periodic high pressure loading.

ACKNOWLEDGEMENT

The support of the Italian MIUR within the Cofin2005 programme “Interfacial resistance and failure in materials and structural systems” is gratefully acknowledged.

REFERENCES

[1] M. W. Carson and M. R. Roach. The strength of the aorta media and its role in the propagation of aortic dissection. *Journal of Biomechanics*, 23:579–588, 1990.

[2] A. Ferrara and A. Pandolfi. Numerical modelling of fracture of human arteries. *Computer Methods in Biomechanics and Biomedical Engineering*, 2008.

[3] G. A. Holzapfel, T. C. Gasser, and R. W. Ogden. A new constitutive framework for arterial wall mechanics and a comparative study of material models. *Journal of Elasticity*, 61(1):1–48, 2000.

[4] G. A. Holzapfel and G. Sommer. Anisotropic mechanical properties of tissue components in human atherosclerotic plaques. *Journal of Biomechanical Engineering*, 126:657–665, 2004.

[5] M. Ortiz and A. Pandolfi. Finite-deformation irreversible cohesive elements for three-dimensional crack-propagation analysis. *International Journal for Numerical Methods in Engineering*, 44:1267–1282, 1999.

[6] A. Pandolfi and M. Ortiz. An efficient adaptive procedure for three-dimensional fragmentation simulations. *Engineering with Computers*, 28:148–159, 2002.

[7] P. Purslow. Positional variations in fracture toughness, stiffness and strength of descending thoracic pig aorta. *Journal of Biomechanics*, 16:947–955, 1983.

[8] A. J. M. Spencer. *Deformation of fiber-reinforced materials*. Oxford University Press, Oxford, 1982.

[9] F. Yang, G. Holzapfel, C. Schulze-Bauer, R. Stollberger, D. Thedens, L. Bolinger, A. Stolpen, and M. Sonka. Segmentation of wall and plaque in in vitro vascular mr images. *The International Journal of Cardiovascular Imaging*, 19:419–428, 2003.

[10] C. Yu, A. Pandolfi, M. Ortiz, D. Coker, and A.J. Rosakis. Three-dimensional modeling of intersonic crack-growth in asymmetrically loaded unidirectional composite plates. *International Journal of Solids and Structures*, 39:6135–6157, 2002.